

This is a repository copy of *Neutron polarisation transfer, $C_{x'}^n$, in π^+ photoproduction off the proton.*

White Rose Research Online URL for this paper:

<https://eprints.whiterose.ac.uk/200241/>

Preprint:

(2022) Neutron polarisation transfer, $C_{x'}^n$, in π^+ photoproduction off the proton.
[Preprint]

Reuse

Items deposited in White Rose Research Online are protected by copyright, with all rights reserved unless indicated otherwise. They may be downloaded and/or printed for private study, or other acts as permitted by national copyright laws. The publisher or other rights holders may allow further reproduction and re-use of the full text version. This is indicated by the licence information on the White Rose Research Online record for the item.

Takedown

If you consider content in White Rose Research Online to be in breach of UK law, please notify us by emailing eprints@whiterose.ac.uk including the URL of the record and the reason for the withdrawal request.

Neutron polarisation transfer, $C_{\chi'}^n$, in π^+ photoproduction off the proton

M. Bashkanov^a, D.P. Watts^a, S.J.D. Kay^b, S. Abt^c, P. Achenbach^f, P. Adlarson^f, F. Afzal^g, Z. Ahmed^b, C.S. Akondi^c, J.R.M. Annand^d, R. Beck^g, M. Biroth^f, N. Borisov^h, A. Braghieriⁱ, W.J. Briscoe^j, F. Cividini^f, C. Collicott^k, S. Costanza^{l,i}, A. Denig^f, E.J. Downie^j, P. Drexler^{m,f}, S. Fegan^a, A. Fix^v, S. Gardner^d, D. Ghosal^e, D.I. Glazier^d, I. Gorodnov^h, W. Gradl^f, D. Gurevichⁿ, L. Heijmanskjöld^f, D. Hornidge^o, G.M. Huber^b, V.L. Kashevarov^{f,h}, M. Korolija^p, B. Krusche^e, A. Lazarev^h, K. Livingston^d, S. Lutterer^e, I.J.D. MacGregor^d, D.M. Manley^c, P.P. Martel^{f,o}, R. Miskimen^q, E. Mornacchi^f, C. Mullen^d, A. Neganov^h, A. Neiser^f, M. Ostrick^f, P.B. Otte^f, D. Paudyal^b, P. Pedroniⁱ, T. Rostomyan^l, V. Sokhoyan^f, K. Spieker^g, O. Steffen^f, I.I. Strakovsky^j, T. Strub^e, I. Supek^p, A. Thiel^g, M. Thiel^f, A. Thomas^f, Yu.A. Usov^h, S. Wagner^f, N.K. Walford^e, J. Wettig^f, M. Wolfes^f, N. Zachariou^a

^aDepartment of Physics, University of York, Heslington, York, YO10 5DD, UK

^bUniversity of Regina, Regina, SK S4S-0A2 Canada

^cKent State University, Kent, Ohio 44242, USA

^dSUPA School of Physics and Astronomy, University of Glasgow, Glasgow, G12 8QQ, UK

^eDepartment of Physics, University of Basel, CH-4056 Basel, Switzerland

^fInstitut für Kernphysik, University of Mainz, D-55099 Mainz, Germany

^gHelmholtz-Institut für Strahlen- und Kernphysik, University Bonn, D-53115 Bonn, Germany

^hJoint Institute for Nuclear Research, 141980 Dubna, Russia

ⁱINFN Sezione di Pavia, I-27100 Pavia, Pavia, Italy

^jCenter for Nuclear Studies, The George Washington University, Washington, DC 20052, USA

^kDepartment of Astronomy and Physics, Saint Mary's University, E4L1E6 Halifax, Canada

^lDipartimento di Fisica, Università di Pavia, I-27100 Pavia, Italy

^mII. Physikalisches Institut, University of Giessen, D-35392 Giessen, Germany

ⁿInstitute for Nuclear Research, RU-125047 Moscow, Russia

^oMount Allison University, Sackville, New Brunswick E4L1E6, Canada

^pRudjer Boskovic Institute, HR-10000 Zagreb, Croatia

^qUniversity of Massachusetts, Amherst, Massachusetts 01003, USA

^rUniversity of California Los Angeles, Los Angeles, California 90095-1547, USA

^sRacah Institute of Physics, Hebrew University of Jerusalem, Jerusalem 91904, Israel

^tDepartment of Physics and Astronomy, Rutgers University, Piscataway, New Jersey, 08854-8019

^uJefferson Lab, 12000 Jefferson Ave., Newport News, VA 23606, USA

^vTomsk Polytechnic University, 634034 Tomsk, Russia

arXiv:2211.09688v1 [nucl-ex] 17 Nov 2022

Abstract

We report a first measurement of the double-polarisation observable, $C_{\chi'}$, in π^+ photoproduction off the proton. The $C_{\chi'}$ double-polarisation observable represents the transfer of polarisation from a circularly polarised photon beam to the recoiling neutron. The MAMI circularly polarised photon beam impinged on a liquid deuterium target cell, with reaction products detected in the Crystal Ball calorimeter. Ancillary apparatus surrounding the target provided tracking, particle identification and determination of recoil nucleon polarisation. The $C_{\chi'}$ observable is determined for photon energies 800-1400 MeV, providing new constraints on models aiming to elucidate the spectrum and properties of nucleon resonances. This is the first determination of any polarisation observable from the beam-recoil group of observables for this reaction, providing a valuable constraint and systematic check of the current solutions of partial wave analysis based theoretical models.

Keywords: photoproduction

1. Introduction

Photoinduced reactions on proton and neutron targets have played a key role in progressing our knowledge of the excited nucleon spectrum the past decade [1], catalysed by quality nucleon photoproduction data from MAMI, JLAB, ELSA and other facilities [2]. These have provided a step change in the

number of measured observables, statistical accuracy, and kinematic coverage.

Pion photoproduction is the simplest photoinduced reaction on the nucleon. The reaction can be described theoretically with four complex amplitudes, which can be fully constrained by kinematically complete measurements of a chosen set of eight observables taken from the cross section, single polarisation observables (where the polarisation of either photon beam, target or recoiling nucleon is determined) and double-polarisation observables formed from simultaneous determination of two of

*Corresponding author

Email address: mikhail.bashkanov@york.ac.uk (M. Bashkanov)

the above polarisation quantities. Recent work has indicated that the properties of the different partial waves in the reaction may converge with fewer measurements than the mathematically complete eight, as discussed in Ref. [3].

Previous double-polarisation measurements for $n\pi^+$ photoproduction are limited to the beam-target group of observables. Measurements of the G observable (linearly polarised beam and transversely polarised target) [6], the E observable (circularly polarised beam and longitudinally polarised target [7]) and more limited data sets for H (circularly polarised beam and transversely polarised target) have recently been obtained [10, 20]. These double-polarisation data, combined with the cross section and single polarisation observables (Σ , T and P) [6, 8] comprise the current world data base.

The lack of any double-polarisation measurements from the beam-recoil group for this channel mean the mathematically "complete" constraint has not been achieved. This lack of previous data reflects the challenges in measurement of recoil nucleon polarisation, requiring a secondary rescattering of the ejectile nucleon in a spin-analysing polarimeter material. Such measurements are only feasible at high photon beam intensities¹. The new C_x data presented here therefore provide an important cross check of convergence in the model predictions. Observables from the beam-recoil group give different sensitivities to the underlying reaction amplitudes, so even if determined with less precision than the beam-target measurements which dominate the database, they have the potential to provide important information on the road to convergence in the model predictions. Some constraint on systematics in both the reaction modelling and the fitted database can also be achieved as C_x is obtained with very different systematics to the beam-target double-polarisation data.²

The photoproduction of $p\pi^0$ is the sister reaction to $n\pi^+$. For the $p\pi^0$ reaction the database is more complete. The differential cross-section, Σ , P , T , G , H , C_x observables have been determined over the full energy range of the new data and E , O_x , O_z for part of the range. Such $p\pi^0$ data are simultaneously fitted by theoretical models along with the $n\pi^+$ data. In combination, sensitivities to the isospin of the contributing nucleon resonances and backgrounds can be achieved.

The leading models to interpret pion photoproduction data, and infer information on the nucleon resonance spectrum, are the SAID [8] and BnGa [9] frameworks, which are both based on partial wave analysis (PWA) methods fitted to the data. The latest iterations of these models (SAID MA19 and BnGa BG2019) experienced substantial change due to the inclusion of new data on the double-polarisation observable G , recently measured at CLAS [6].

¹To achieve such measurements around four orders of magnitude larger statistics are required than for a typical beam-target measurements as only $\sim 2\%$ of the ejected events can be analysed with a practical thickness of nucleon scattering medium.

²For example, correlated systematics could potentially arise as all the beam-target observables employed common methodologies in determining the degree of linear beam polarisation and MAMI/ELSA had common polarised target systems.

In this work we make a first determination of the C_x observable for the $p(\gamma^\circ, \vec{n}\pi^+)$ reaction. This is the first measurement of any observable from the beam-recoil double polarisation group for this reaction and the results are compared to nearly converged predictions from the leading partial wave analysis based theoretical models. The C_x observable is extracted using a bootstrap statistical technique which gives access to statistical and systematic errors in a robust way. We compare the new data to the SAID [8] and BnGa [9] models, which are fitted to a database currently unconstrained by measurements of beam-recoil observables in this reaction channel.

2. Experimental details

The measurement employed a new, large acceptance, neutron polarimeter [11] within the Crystal Ball detector at the A2@MAMI [12] facility during a 300 hour beamtime. A 1557 MeV longitudinally polarised electron beam impinged on either a thin amorphous (cobalt-iron alloy) or crystalline (diamond) radiator, producing circularly (alloy) or elliptically (diamond) polarised bremsstrahlung photons. The electron helicity was regularly flipped to produce a photon beam with equal amounts of both circular photon polarisations. As linear photon beam polarisation is not used to extract C_x^n , equal flux from the two elliptical polarisation settings were combined to increase the circularly polarised photon yield³. The photons were energy-tagged ($\Delta E \sim 2$ MeV) by the Glasgow-Mainz Tagger [13] and impinged on a 10 cm long liquid deuterium target cell. Reaction products were detected by the Crystal Ball (CB) [14], a highly segmented NaI(Tl) photon calorimeter covering nearly 96% of 4π steradians. For this experiment, a new bespoke 24 element, 7 cm diameter and 30 cm long plastic scintillator barrel (PID-POL) [15] surrounded the target, with a smaller diameter than the earlier PID detector [15], but which provided similar particle identification capabilities. A 2.6 cm thick cylinder of analysing material (graphite) for nucleon polarimetry was placed around PID-POL, covering polar angles $12^\circ < \Theta < 150^\circ$ and occupying the space between PID-POL and the Multi Wire Proportional Chamber (MWPC) [16]. The MWPC provided charged particle tracking for particles passing out of the graphite into the CB. At forward angles, an additional 2.6 cm thick graphite disk covered the range $2 < \Theta < 12^\circ$ [15, 17, 18]. A GEANT4 visualisation of the experimental setup can be seen in Fig. 1.

The cryogenic deuterium target provided a source of weakly bound protons and neutrons. The $d(\gamma, \pi^+ \vec{n})n_{spec}$ events of interest consist of a primary charged pion track and a reconstructed neutron, which undergoes a (n, p) charge-exchange reaction in the graphite to produce a secondary proton; the spectator neutron is not detected. The secondary proton gives signals in the MWPC and CB. The primary π^+ was identified using the correlation between the energy deposits in the PID and CB using

³Separate treatment of the events with two elliptical photon polarisations and with pure circular photon polarisation, gave consistent results within the achievable statistical accuracy.

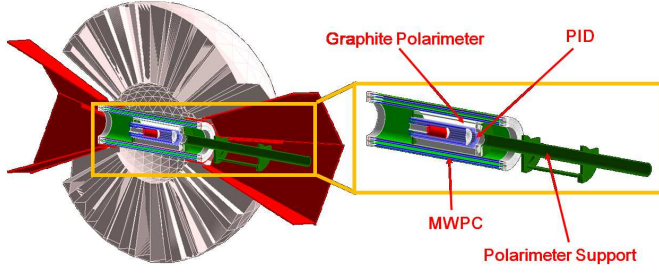


Figure 1: Crystal Ball setup during the polarimeter beamtime. The cryogenic target (red cell) is surrounded by the PID barrel (blue), the graphite polarimeter (grey), the MWPC (blue/green) and the Crystal Ball (white).

$\Delta E - E$ analysis [15] along with an associated charged track in the MWPC. The intercept of the primary π^+ track with the photon beamline allowed determination of the production vertex, and hence permitted the yield originating from the target cell windows to be removed. Neutron $^{12}\text{C}(n, p)$ charge exchange candidates required an absence of a PID-POL signal on the reconstructed neutron path, while having an associated track in the MWPC and signal in the CB from the scattered secondary proton. The incident neutron angle (Θ_n) was determined from reaction kinematics using E_γ and the production vertex coordinates. A distance of closest approach condition was imposed to ensure a crossing of the (reconstructed) neutron track and the secondary proton candidate track (measured with MWPC and CB). Once candidate pion and neutron tracks were identified, a kinematic fit was employed to increase the purity of the data sample and improve the determination of the reaction kinematics (see Ref [19] for details).

3. Determination of C_x^n

The transferred neutron polarisation (C_x^n) was determined through analysis of the neutron-spin dependent $^{12}\text{C}(n, p)$ reactions occurring in the graphite polarimeter. The spin-orbit component of the nucleon-nucleon interaction results in a ϕ -anisotropy in the produced yield of secondary protons (see Ref. [20] for details). We followed the same procedure to determine C_x^n , as described in Ref. [18], where the same observable was extracted for the deuteron photodisintegration reaction. The C_x^n extraction employs a combination of log-likelihood and bootstrap techniques, as discussed below. The likelihood was defined as

$$L_i = c_i \left[1 + C_x^n \cdot P_{\gamma,i}^\circ \cdot A_{y,i} \cdot \sin(\phi_i^{scat}) \right] A, \quad (1)$$

where c_i is a normalisation coefficient, A is the detector acceptance, C_x^n is the spin transfer observable of interest, $P_{\gamma,i}^\circ$ is the degree of photon circular polarisation, $A_{y,i}$ is the neutron analysing power⁴ and ϕ^{scat} is the ϕ scattering angle in the

⁴ $P_{\gamma,i}^\circ$ is photon energy dependent and A_y depends on the ejected neutron energy and scattered proton polar angle. Both variables are evaluated on an event-by-event basis.

primed frame, see Fig. 2. The log-likelihood function that was maximised to obtain the observable of interest is given by

$$\log L = b + \sum_i \log \left[1 + C_x^n \cdot P_{\gamma,i}^\circ \cdot A_{y,i} \cdot \sin(\phi_i^{scat}) \right], \quad (2)$$

where the constant b is an observable-independent constant, which absorbs the normalisation coefficient and detector acceptance. The summation (i) runs over all events. To reduce systematic dependencies, the events were only retained if $A_y(np)$ was above 0.1, and the proton scattering angle was in the range $\Theta_p^{scat} \in 15 - 45^\circ$, where Θ_p^{scat} is the polar angle of the scattered proton relative to the direction of the neutron. The above cuts restrict the kinetic energy of the neutrons to be above 200 MeV, as well as their polar angle, Θ_n , to be larger than $\sim 40^\circ$, allowing them to be well within the acceptance of the polarimeter. Events meeting the conditions required a photon energy larger than 800 MeV and neutron centre-of-mass angle close to 90° .

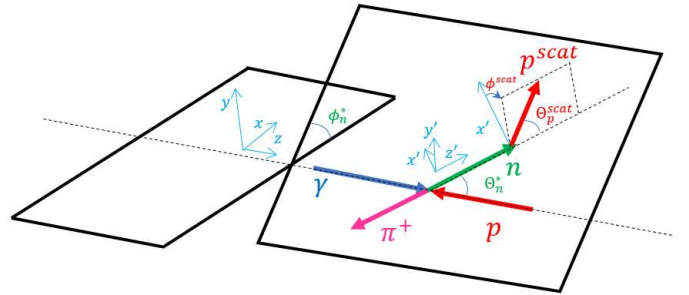


Figure 2: Kinematics of the reaction in the centre-of-mass system. The z-axis is oriented along the photon beam, the y-axis is vertically upwards in the laboratory; the z' -axis is oriented along the ejectile neutron direction, and the y' -axis is perpendicular to the reaction plane.

The extraction of C_x^n is simpler than the previous extraction of P_y due to cancellations in the acceptance.⁵ A regular (~ 1 s) flipping of the photon helicity allowed us to reduce systematic effects associated with a temporal variation of the detector acceptance to negligible values. In addition, in the determination of the C_x^n observable, the acceptance effects completely factor-out in the likelihood extraction (unlike the extraction of P_y). The use of an unbinned (in ϕ and E_γ) likelihood method eliminates bin-size related systematics arising from fits of trigonometric functions to binned ϕ^{scat} -asymmetries.

The spin transfer observable, $C_x^n = f(\Theta_n^*, E_\gamma)$, was determined in 10° neutron centre-of-mass (CM) angle bins using a likelihood-extraction in which a smooth energy dependence is assumed. To get robust error evaluations within the likelihood method we employed a bootstrap procedure [21]. This method involves randomly selecting N events out of our sample of N events allowing repetitions⁶. For each combination, a likeli-

⁵The determination of P_y is obtained from a $(\cos(\phi_i^{scat}))$ dependence, which is sensitive to any systematics between forward and backward angle scattering [17]. In contrast, C_x^n has a $(\sin(\phi_i^{scat}))$ dependence (left-right asymmetry) for which the cylindrically symmetrical A2 setup has minimal acceptance/efficiency effects.

⁶For example, in the case of the 80° bin it is 9200 random events out of a 9200 event sample.

hood fit is carried out to extract $C_{x'}^n$. Each fit produces a smooth function $C_{x'}^n = f(E_\gamma)$ for the given Θ_n bin. Multiple repetitions of this procedure enable determination of the most likely $C_{x'}$ and its associated errors $C_{x'}^n$. These are presented in Fig. 3 (middle). Additional studies of systematic effects were obtained by relaxing the analysis cuts. The systematic errors are extracted from the resulting variations in the extracted values of $C_{x'}$. The magnitude of the systematic errors in each bin are influenced by the achievable statistical accuracy in the bin. The extracted systematic errors are also shown in Fig. 3 (bottom)⁷.

4. Results

Our $C_{x'}^n$ results, along with associated statistical and estimated systematic errors, are presented in Fig. 3 as a function of photon energy and neutron CM polar angle. The new data cover photon energy bins from 800 MeV up to 1400 MeV and CM angles for the neutron of 70-120°. The magnitude of $C_{x'}^n$ is seen to be small over much of the sampled phase space, albeit with indications of localised regions of both high and low $C_{x'}^n$. The statistical and systematic uncertainties are both largely uniform over much of the phase space, but with expected deterioration close to the edge of the polarimeter acceptance.

Example comparisons of the new data with recent solutions of the SAID [8] and BnGa [6] partial wave fits are shown in Fig. 4 and 5. In Fig. 4 the data are presented as a function of photon energy for a fixed angular bin of 80°. For photon energies up to 1200 MeV the data are well described by all SAID and BnGa solutions (see figure caption) within the achievable experimental errors⁸. Above this, the data may suggest higher $C_{x'}^n$ than both model predictions - albeit in regions where the estimated systematic uncertainties are large.

The angular distribution of $C_{x'}^n$ at 1100 MeV is presented in Fig. 5 (top), compared to the model predictions. The observed zero crossing at around 90° is broadly consistent with all model predictions, however the second crossing around 108° is in better agreement with the latest BnGa solution. The angular distribution of $C_{x'}^n$ at 1200 MeV, Fig. 5 (bottom), shows a broadly similar shape to the lower energy bin, but with indications of regions of higher positive $C_{x'}^n$. The divergence between the models is larger for this higher photon energy bin. The most recent SAID and BnGa fits (red solid and red-dashed respectively) include the large new G^- dataset [6] for $n\pi^+$, but its inclusion results in both models giving a poorer description of this independent $C_{x'}^n$ variable. This suggests constraint from a different double-polarisation group, even with poorer coverage and accuracy, has the potential to provide new information. Future fits including the new data may improve convergence between the models for this photon energy region.

The statistical and systematic uncertainties in $C_{x'}^n$ extraction could be significantly reduced in the future due to recent upgrades in the MAMI beam intensity. Accurate beam-recoil data

⁷The dataset corresponds to kinematical regions where $C_{x'}^n$ statistical errors are less than 0.5 or systematic errors are smaller than 0.8.

⁸The structure seen in theory curves around $E_\gamma \sim 700$ MeV originates from the η -meson production threshold.

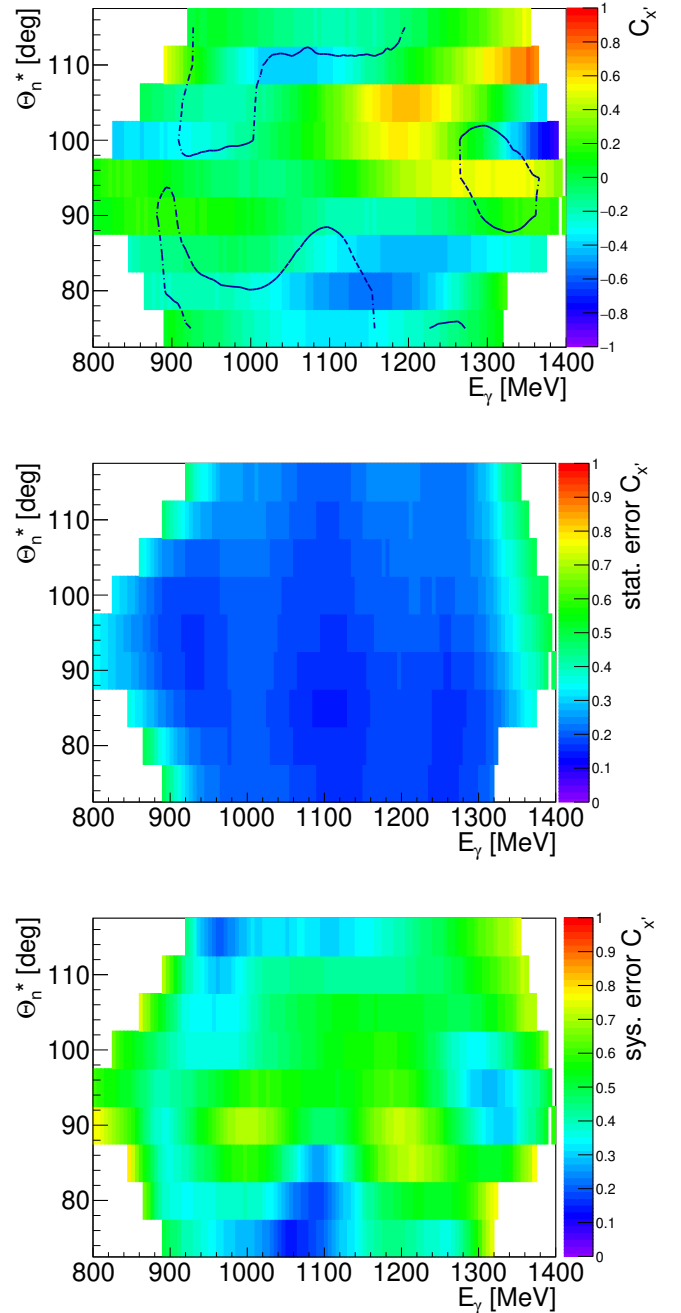


Figure 3: Two-dimensional $C_{x'}^n$ dependence as a function of neutron centre-of-mass angle, Θ_n^* and photon energy E_γ (top), statistical (middle) and systematic (bottom) uncertainties for this distribution. Systematic uncertainty contour lines at 0.4 are also shown on the top plot as dash-dot lines.

appears important even when, as is the case here, an extensive database of beam-target double-polarisation observables has already been obtained.

- [11] D.P. Watts, J.R.M Annand, M. Bashkanov, D.I Glazier, MAMI Proposal Nr. A2/03-09, http://bamboo.pv.infn.it/Mambo/MAMI/prop_2009/MAMI-A2-03-09.pdf
- [12] K.-H. Kaiser *et al.*, Nucl. Instr. Meth. A **593**, 159 (2008).
- [13] J.C. McGeorge *et al.*, Eur. Phys. J. A **37**, 129 (2008).
- [14] A. Starostin *et al.*, Phys. Rev. C **64**, 055205 (2001).
- [15] S.J.D. Kay, Ph.D. thesis, University of Edinburgh, 2018.
- [16] G. Audit *et al.* Nucl. Instr. Meth. A **301**, 473, (1991).
- [17] M. Bashkanov *et al.*, Phys. Rev. Lett. **124**, 132001, (2020).
- [18] M. Bashkanov *et al.*, arXiv:2206.12299
- [19] M. Bashkanov *et al.*, Phys. Lett. B **789**, 7, (2019).
- [20] SAID database <http://gwdac.phys.gwu.edu/>; R. A. Arndt *et al.*, Phys. Rev. C **76**, 025209, (2007).
- [21] A. Pastore, J. Phys. G, **46**, 052001, (2019).
- [22] Ron L. Workman *et al.*, Phys. Rev. C **86**, 015202, (2012)
- [23] <https://doi.org/10.15124/53c8fd02-4b3f-4fb9-908e-60c487d5615b>